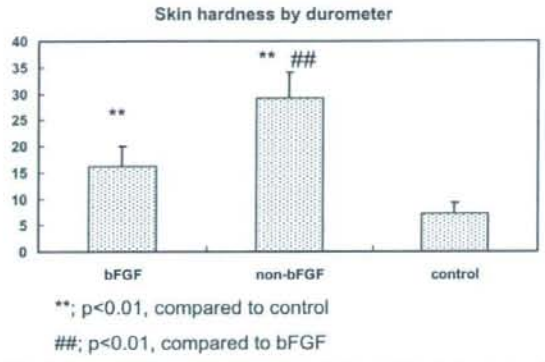

Fig. 1. *The relative value of the durometer reading was compared among groups. The values were 16.2 ± 3.83, 29.2 ± 4.94, and 7.2 ± 2.03, bFGF-treated, non-bFGF-treated and control groups, respectively (p < 0.01 between non-bFGF-treated vs. bFGF-treated and control groups).*

One patient (case 7) had been reconstructed with artificial dermis and subsequent split-thickness skin grafting the previous year in the right extremity, and the other side was reconstructed with bFGF and artificial dermis as bFGF was clinically permitted for use from 2001 in Japan.

Skin Hardness by Duromer

Skin hardness measured using a durometer demonstrated significant differences among groups. The relative value of the actual durometer reading was lowest in the control group, which is nonwounded skin. bFGF treatment together with the artificial dermis was the next lowest and the artificial dermis alone demonstrated the highest value (7.2 ± 2.03, 16.2 ± 3.83, 29.2 ± 4.94, control, bFGF, non-bFGF, respectively, $p < 0.01$) (Fig. 1).

Skin Moisture Analysis

For moisture meter analyses, the effective contact coefficient was significantly higher compared with the nonwounded skin value (control) in both bFGF and non-bFGF-treated artificial dermis groups, and there was a significant difference between bFGF- and non-bFGF-treated groups (10.9% ± 1.05%, 17.9% ± 1.95%, 4.4% ± 0.85%, bFGF, non-bFGF and nonwounded skin (control) groups, respectively, $p < 0.01$). TEWL in the bFGF-treated group was significantly less than that in the non-bFGF group (13.2 ± 2.16 g/m^2/h, 21.2 ± 2.93 g/m^2/h; bFGF treated, non-bFGF treated, respectively, $p < 0.01$). The bFGF-treated group demonstrated a significantly higher TEWL value compared with the control (13.2 ± 2.16 g/m^2/h, 6.3 ± 1.10 g/m^2/h; bFGF treated, control, respectively, $p < 0.01$). The correlation between the effective contact coefficient and TEWL demonstrated significant correlation between the two ($y = 0.81x + 0.053$, $r^2 = 0.86$, $p < 0.01$).

Table 3 Skin Moisture Meter Analysis

	bFGF (n = 12)	Non-bFGF (n = 7)	Non-Wounded (control, n = 20)
Effective contact coefficient (%)	10.9 ± 1.05*	17.9 ± 1.95*†	4.4 ± 0.85
Transepidermal water loss (TEWL) (g/m^2/h)	13.2 ± 2.16*	21.2 ± 2.93*†	6.3 ± 1.10
Water content (μS)	24.7 ± 5.06	46.0 ± 5.67*†	23.5 ± 4.42
Thickness (μm)	12.1 ± 3.14	17.2 ± 1.87*†	10.5 ± 1.62

* $p < 0.01$, compared to control.
† $p < 0.01$, compared to bFGF.

The water content in the non-bFGF group was significantly greater than the bFGF-treated and control groups, whereas there was no significant difference between the bFGF-treated and the control groups (24.7 ± 5.06 μS, 46.0 ± 5.67 μS, 23.5 ± 4.42 μS; bFGF-treated, non-bFGF-treated, control groups, respectively, $p < 0.01$; between control and non-bFGF-treated groups and between bFGF-treated and non-bFGF-treated groups). The thickness of the non-bFGF-treated group was significantly greater than both the control and bFGF-treated groups (12.1 ± 3.14 μm, 17.2 ± 1.87 μm, 10.5 ± 1.62 μm; bFGF-treated, non-bFGF-treated, control groups, respectively, $p < 0.01$) (Table 3). Anatomic locations of the moisture meter and the measurement conditions were similar among three groups.

Case Presentation

An 80-year-old woman was suddenly developed her left calf cellulitis, which caused her emergency debridement of the skin and subcutaneous tissues at Nagasaki University hospital by an orthopedic surgeon on duty. She was then referred to us for further leg reconstruction. There was 1×10^6 CFU/mL of Methicillin-Resistant *Staphylococcus aureus* in wound surface by a swab bacterial culture. Additionally more meticulous debridement including the partial fascia and periosteum in her anterior calf was performed 10 days after initial debridement on her calf and bFGF was sprayed over the wound bed after hemostasis, about 1000 μg of bFGF was sprayed over the wound bed, then an artificial dermis was applied over entire defects. Daily 100 μg of bFGF was needle inserted beneath outer membrane of the artificial dermis. In 2 weeks, 0.012-inch split-thickness skin grafting was placed. In 3 years, a pretibial durometer reading is as low as 18.3, and TEWL demonstrated 23.5 g/m^2/h and thickness of the stratum corneum was 11.5 μm (Fig. 2).

DISCUSSION

Staged lower extremity reconstruction with daily bFGF-treated artificial dermis and subsequently thinner split-thickness skin grafting was beneficial for the quality of reconstructed skin in comparison with the artificial dermis and split-thickness skin grafting alone in terms of hardness and moisture parameters such as TEWL, water content and thickness. The bFGF-

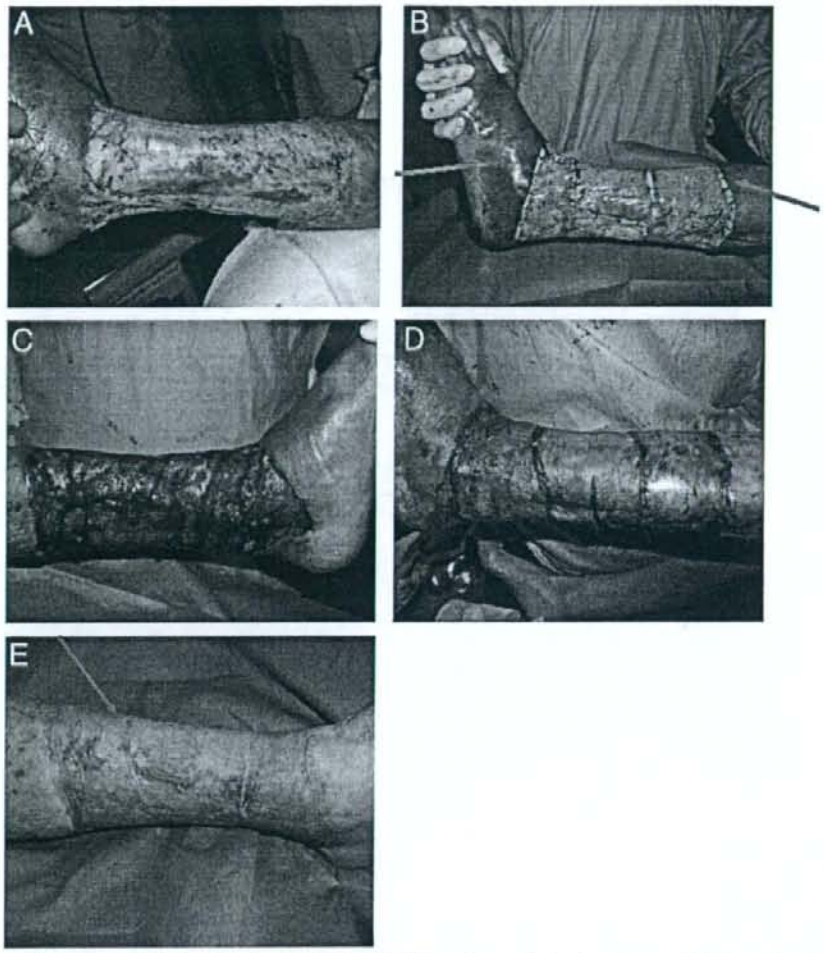

Fig. 2. *An 80-year-old woman suddenly developed calf cellulitis.* (A) *When she was first referred to us at 10 days after primary debridement by an orthopedic surgeon.* (B) *After careful hemostasis and 1000 μg of bFGF over the wound bed was sprayed and then an artificial dermis (Pelnac) was covered. From the arrows by needles, total 100 μg of bFGF was administered daily until secondary split-skin grafting.* (C) *In 14 days after the artificial dermis and daily bFGF application.* (D) *At time of 0.012-inch split-skin grafting was performed.* (E) *In 3 years after skin grafting. The pretibial durometer reading demonstrated 18.3 at half a year and 18.5 at 3 years where the periosteum has to be removed.*

treated reconstruction demonstrated almost equal values in water content and thickness, consistent with the softer and thus better nature of the reconstructed lower extremity.

Analysis using a durometer successfully demonstrated a positive correlation with clinical skin hardness severity scores when split-skin grafting was performed with or without bFGF.[23] In this study, there was a significantly high value for non-bFGF artificial dermis reconstruction compared with control (normal skin) and bFGF-treated artificial dermis reconstruction. The relative ratio of a durometer value in the previous skin grafting study was 1:2 (bFGF-treated vs. non-bFGF-treated skin grafting). In staged artificial dermis with or without bFGF-treated skin grafting, it preserved almost the similar ratio, 1:1.8 (bFGF-treated vs. non-bFGF-treated). This may account for how well the primary content of collagen in the artificial dermis sustained applied bFGF in the wound bed and further affected skin remodeling through skin grafting. In fact, there was a report on the possible function of type I collagen as a reservoir of bFGF in a murine model of the subcutis, intramuscular injection, and ischemic hind limb.[26] Analysis using a moisture meter enabled the evaluation of corneal layer (stratum corneum) functions by the

effective contact coefficient, together with TEWL, water content, and layer thickness. Abnormal functioning of corneal layers is well demonstrated in atopic dry skin studies by such as increased TEWL, decreased water content, and increased thickness as the atopic dry skin thickens. As atopic skin decreases the amount of intercellular phospholipids or ceramides, this may account for the damaged function of the corneal layers.[27] In wounded skin, deeper wounds, hypertrophic scars and keloids demonstrated high TEWL and water content values. These data also suggest that proliferative changes in the dermis may affect the corneal layers.

In our study, there was a significantly higher value of TEWL in the non-bFGF-treated group than the bFGF-treated and control groups, and the bFGF-treated group demonstrated significantly higher TEWL than the control. The water content was significantly greater in the non-bFGF-treated group than the control: the bFGF-treated group was comparable with the control and this value was significantly lower than that of the non-bFGF-treated group ($p < 0.01$). bFGF-treated reconstruction may offer better skin remodeling as early as immediately after debridement, which may avoid the development of fibro-proliferative disorders.[28] As the frequency of tape-stripping increases, the water-holding defects of the corneal layers (stratum corneum) are associated with a higher value of TEWL.[29] Thus, TEWL is an important marker of hydration for epithelialization or re-epithelialization after healing. The effective contact coefficient is affected by skin surface electrolytes such as sweating; however, this value also reflects the barrier function of the skin. In our study, there was a correlation between the effective contact coefficient and TEWL. The strongly positive correlation between effective contact coefficient and TEWL demonstrates the higher validity of the moisture measurement. The thickness in both the bFGF-treated and control groups was significantly smaller than that in the non-bFGF-treated group.

Overall, bFGF-treated sequential artificial dermis and skin grafting demonstrated better scarring and well-organized stratum corneum after healing both by durometer and moisture meter analysis.

The advantage of using an artificial dermis includes immediate coverage for deeper tissue exposure such as tendon and bone, protecting from fluid, protein, and electrolyte loss, from microorganism invasion and reducing secondary donor-site morbidity as only thinner skin grafting is required.[19] Also, the combination of artificial dermis with bFGF demonstrated the reconstruction of deep diabetic soft tissue loss,[21] diabetic pressure ulcer healing in a mouse model,[22] and intractable fingertip ulcers caused by burn injury.[20]

Even in larger tissue defects as demonstrated in case 6 of 50×35 cm^2 that are too difficult to cover using the conventional method, or when donor skin is limited, this combination procedure using artificial dermis and bFGF may be useful. In addition, when subsequent or additional debridement is required, donor-site morbidity is minimal and a semi-transparent membrane may be easier to evaluate. The use of a porcine-derived artificial dermis in the lower extremities with daily bFGF administration is easy, safe and useful although secondary split-thickness skin grafting is required and the reconstructed outcome is better in quality.

REFERENCES

1. Henke PK, Blackburn SA, Wainess RW, et al. Osteomyelitis of the foot and toe in adults is a surgical disease: conservative management worsens lower extremity salvage. *Ann Surg.* 2005;241:885–892.
2. Khammash MR, Obeidat KA. Prevalence of ischemia in diabetic foot infection. *World J Surg.* 2003;27:797–799.
3. Patel GK. The role of nutrition in the management of lower extremity wounds. *Int J Low Extrem Wounds.* 2005;4:12–22.
4. Kauffman CA, Lahoda LU, Cederna PS, et al. Use of soleus muscle flaps for coverage of distal third tibial defects. *J Reconstr Microsurg.* 2004;20:593–597.
5. Maloney CT Jr, Wages D, Upton J, et al. Free omental tissue transfer for extremity coverage and revascularization. *Plast Reconstr Surg.* 2003;111:1899–1904.
6. Thomas TA, Taylor SM, Crane MM, et al. An analysis of limb-threatening lower extremity wound complications after 1090 consecutive coronary artery bypass procedures. *Vas Med.* 1999;4:83–88.
7. Hom DB, Manivel JC. Promoting healing with recombinant human platelet-derived growth factor-BB in a previously irradiated problem wound. *Laryngoscope.* 2003;113:1566–1571.
8. Palmer-Kazen U, Wariaro D, Luo F, et al. Vascular endothelial cell growth factor and fibroblast growth factor 2 expression in patients with critical limb ischemia. *J Vasc Surg.* 2004;39:621–628.
9. Steed DL. Clinical evaluation of recombinant human platelet-derived growth factor for the treatment of lower extremity diabetic ulcers. Diabetic Ulcer Study Group. *J Vasc Surg.* 1995;21:71–78.
10. Wieman TJ, Smiell JM, Su Y. Efficacy and safety of a topical gel formulation of recombinant human platelet-derived growth factor-BB (becaplermin) in patients with chronic neuropathic diabetic ulcers. A phase III randomized placebo-controlled double-blind study. *Diabetes Care.* 1998;21:822–827.
11. Nayeri F, Olsson H, Peterson C, et al. Hepatocyte growth factor; expression, concentration and biological activity in chronic leg ulcers. *J Dermatol Sci.* 2005;37:75–85.
12. Bianchi L, Ginebri A, Hagman JH, et al. Local treatment of chronic cutaneous leg ulcers with recombinant human granulocyte-macrophage colony-stimulating factor. *J Eur Acad Dermatol Venereol.* 2002;16:595–598.
13. Cruciani M, Lipsky BA, Mengoli C, et al. Are granulocyte colony-stimulating factors beneficial in treating diabetic foot infections? A meta-analysis. *Diabetes Care.* 2005;28:454–460.
14. Fu X, Shen Z, Guo Z, et al. Healing of chronic cutaneous wounds by topical treatment with basic fibroblast growth factor. *Chin Med J (Engl).* 2002;115:331–335.
15. Richard JL, Parer-Richard C, Daures JP, et al. Effect of topical basic fibroblast growth factor on the healing of chronic diabetic neuropathic ulcer of the foot. A pilot, randomized, double-blind, placebo-controlled study. *Diabetes Care.* 1995;18:64–69.
16. Ferguson MW, O'Kane S. Scar-free healing: from embryonic mechanisms to adult therapeutic intervention. *Philos Trans R Soc Lond B Biol Sci.* 2004;359:839–850.
17. Hsu M, Peled ZM, Chin GS, et al. Ontogeny of expression of transforming growth factor-beta 1 (TGF-beta 1), TGF-beta 3, and TGF-beta receptors I and II in fetal rat fibroblasts and skin. *Plast Reconstr Surg.* 2001;107:1787–1794.
18. Beanes SR, Dang C, Soo C, et al. Down-regulation of decorin, a transforming growth factor-beta modulator, is associated with scarless fetal wound healing. *J Pediatr Surg.* 2001;36:1666–1671.

19. Suzuki S, Kawai K, Ashoori F, et al. Long-term follow-up study of artificial dermis composed of outer silicone layer and inner collagen sponge. *Br J Plast Surg.* 2000;53:659–666.
20. Muneuchi G, Suzuki S, Moriue T, et al. Combined treatment using artificial dermis and basic fibroblast growth factor (bFGF) for intractable fingertip ulcers caused by atypical burn injuries. *Burns.* 2005;31:514–517.
21. Ito K, Ito S, Sekine M, et al. Reconstruction of the soft tissue of a deep diabetic foot wound with artificial dermis and recombinant basic fibroblast growth factor. *Plast Reconstr Surg.* 2005;115:567–572.
22. Kawai K, Suzuki S, Tabata Y, et al. Accelerated wound healing through the incorporation of basic fibroblast growth factor-impregnated gelatin microspheres into artificial dermis using a pressure-induced decubitus ulcer model in genetically diabetic mice. *Br J Plast Surg.* 2005;58:1115–1123.
23. Akita S, Akino K, Imaizumi T, et al. A basic fibroblast growth factor improved the quality of skin grafting in burn patients. *Burns.* 2005;31:855–858.
24. Akita S, Tanaka K, Hirano A. Lower extremity reconstruction after necrotizing fasciitis and necrotic skin lesions using a porcine-derived skin substitute. *J Plast Reconstr Aesthet Surg.* 2006;59:759–763.
25. Akita S, Akino K, Imaizumi T, et al. A polyurethane dressing is beneficial for split-thickness skin-graft donor wound healing. *Burns.* 2006;32:447–451.
26. Kanematsu A, Marui A, Yamamoto S, et al. Type I collagen can function as a reservoir of basic fibroblast growth factor. *J Control Release.* 2004;99:281–292.
27. Imokawa G, Abe A, Jin K, et al. Decrease level of ceramides in stratum corneum of atopic dermatitis. *J Invest Dermatol.* 1991; 96:523–526.
28. Rahban SR, Garner WL. Fibroproliferative scars. *Clin Plast Surg.* 2003;30:77–89.
29. Tagami H, Yoshikuni K. Interrelationship between water-barrier and reservoir functions of pathologic stratum corneum. *Arch Dermatol.* 1985;121:642–625.

Basic fibroblast growth factor accelerates and improves second-degree burn wound healing

Sadanori Akita, MD, PhD[1]; Kozo Akino, MD, PhD[2]; Toshifumi Imaizumi, MD[1]; Akiyoshi Hirano, MD[1]

1. Division of Plastic and Reconstructive Surgery, and
2. Division of Anatomy and Neurobiology, Department of Developmental and Reconstructive Medicine, Nagasaki University, Graduate School of Biomedical and Sciences, Nagasaki, Japan

Reprint requests:
Sadanori Akita, MD, PhD, Division of Plastic and Reconstructive Surgery, Nagasaki University, School of Medicine, 1-7-1 Sakamoto machi, Nagasaki, 852-8501, Japan.
Email: akitas@hf.rim.or.jp

Manuscript received: December 21, 2007
Accepted in final form: May 16, 2008

DOI:10.1111/j.1524-475X.2008.00414.x

ABSTRACT

Second-degree burns are sometimes a concern for shortening patient suffering time as well as the therapeutic choice. Thus, adult second-degree burn patients (average 57.8 ± 13.9 years old), mainly with deep dermal burns, were included. Patients receiving topical basic fibroblast growth factor (bFGF) or no bFGF were compared for clinical scar extent, passive scar hardness and elasticity using a Cutometer, direct scar hardness using a durometer, and moisture analysis of the stratum corneum at 1 year after complete wound healing. There was significantly faster wound healing with bFGF, as early as 2.2 ± 0.9 days from the burn injury, compared with non-bFGF use (12.0 ± 2.2 vs. 15.0 ± 2.7 days, $p < 0.01$). Clinical evaluation of Vancouver scale scores showed significant differences between bFGF-treated and non-bFGF–treated scars ($p < 0.01$). Both maximal scar extension and the ratio of scar retraction to maximal scar extension, elasticity, by Cutometer were significantly greater in bFGF-treated scars than non-bFGF–treated scars (0.23 ± 0.10 vs. 0.14 ± 0.06 mm, 0.59 ± 0.20 vs. 0.49 ± 0.15 mm: scar extension, scar elasticity, bFGF vs. non-bFGF, $p < 0.01$). The durometer reading was significantly lower in bFGF-treated scars than in non-bFGF–treated scars (16.2 ± 3.8 vs. 29.3 ± 5.1, $p < 0.01$). Transepidermal water loss, water content, and corneal thickness were significantly less in bFGF-treated than in non-bFGF–treated scars ($p < 0.01$).

Second-degree burns are sometimes a concern as to whether early surgery should be selected or whether it should be delayed until remnant dermal components are reepithelialized. Early excision and grafting of < 20% of the total burn surface area (TBSA) is superior to nonoperative treatment from the viewpoint of hypertrophic scar (HS) formation and scar quality.[1] Recently, dermal replacement template surgery on postburn day 5, followed by auto-grafting on postburn day 21 for patients with deep dermal burns to full-thickness burns were demonstrated as safe and effective treatment modalities for the TBSA, 43% burns.[2] On the other hand, a conservative approach for deep dermal burn wounds using polarized-light irradiation resulted in a shorter healing time, almost no HS, and optimal esthetic and functional outcomes with a relatively long-term follow-up.[3]

Another modality for the treatment of burn wounds, systemic administration of growth hormone, which attenuates pro-inflammatory cytokines such as tumor necrosis factor-α (TNF-α), is beneficial for the metabolism, and may lead to accelerated wound healing at donor sites in patients with large cutaneous burns.[4] Second-degree thermal injuries of rat skin showed the complement-independent involvement of pro-inflammatory cytokines such as interleukin-1 (IL-1), TNF-α, and IL-6 as results of reactive oxygen metabolites generated by neutrophils, which were accumulated in the dermal burn wounds.[5] Another heparin-binding cytokine, midkine, showed enhanced expression as early as day 1 after deep dermal burn injury in a rat model.[6] Continuous recombinant human erythropoietin from 3 hours to 14 days after deep burn injury improved angiogenesis and wound healing in a mouse model by the expression of CD31 endothelial markers and inducible nitric oxide synthases, and the wound content of nitric oxide products and by augmenting vascular endothelial growth factor content.[7] Among cytokines, basic fibroblast growth factor (bFGF) showed endogenous immunolocalization in the human dermis in partial-thickness burns from day 4 to day 11. The bFGF participates in cutaneous wound healing by activating local macrophages up to the remodeling phase, which occurs several weeks after injury.[8] The bFGF in burn wounds may be a presynthesized mediator that is released locally from injury sites, and thus may play an important role in early wound healing.[9] In adult second-degree burns, the topical application of bFGF within 5 days postinjury showed significantly better regeneration of granulation tissues and newly formed capillaries in a randomized-controlled clinical trial.[10] We therefore sought to investigate bFGF in second-degree burns with conventional wound care alone. Objective analyses using a moisture meter for healed epithelial layer (stratum corneum) function, a durometer for scar hardness, and a Cutometer for scar elasticity as well as clinical assessment were compared in bFGF-treated and non-bFGF–treated groups.

Table 1. Patient profiles

	bFGF (n=51)	non-bFGF (n=51)	Control (non-wounded) (n=51)
Sex (F:M)	24:27	21:30	25:26
Age (years)	60.0 ± 10.8	54.4 ± 16.3	58.9 ± 13.9
TBSA (%)	8.9 ± 4.3	9.5 ± 5.0	
Burn type	Scald=33	Scald=31	
	Flame=14	Flame=14	
	Contact=4	Contact=6	
Location			
	Total=119	Total=122	
	Upper extremity=33	Upper extremity=33	
	Lower extremity=34	Lower extremity=33	
	Torso=27	Torso=27	
	Face=25	Face=29	
Healing time (days)	12.0 ± 2.2	15.0 ± 2.7**	

Upper extremity=arm, hand, finger.
Lower extremity=thigh, leg, foot, toe.
Torsochest, back, abdomen.
**$p < 0.01$.

PATIENTS AND METHODS

Patients

We enrolled 153 subjects (22–90 years old; average 57.8 ± 13.9 years of age, 51 with bFGF treatment, 51 with non-bFGF treatment, and 51 age-matched healthy volunteers) in this investigation from November 2001 to March 2006. The bFGF treatment group included 24 female and 27 male patients with an average age of 60.0 ± 10.8 years (40–87 years old), with an average TBSA of 8.9 ± 4.3%. The non-bFGF treatment group included 21 female and 30 male patients with an average age of 54.4 ± 16.3 years (22–89 years old), with an average TBSA of 9.5 ± 5.0% after approval from the internal review board in Nagasaki University Hospital. The patients were randomized by the date of their first visits to our hospital. Patients were treated with bFGF on odd days, while patients who came on even days were included in the non-bFGF–treated group. There was no statistical significance between bFGF and non-bFGF groups in terms of age or TBSA. Other than whether using bFGF or not, all therapeutic regimens were exactly the same between the two groups. For instance, the timing of the dressing changes or use of the ointment-impregnated gauzes from the initial treatment until wound healing was identical.[11] The age-matched volunteers (25 women and 26 men) were patients who visited the hospital for complaints other than scar problems with an average age of 58.9 ± 13.9 years (26–90 years old). There were no significant differences among volunteers, bFGF, and non-bFGF groups.

All burns were diagnosed as second-degree burns. The majority of the burns were deep dermal burns and some were mixed superficial and deep dermal burns at first observed clinically. The burn types were contact (n=4), flame (n=14), and scald (n=33) in the bFGF-treated group, with a similar distribution in the non-bFGF–treated burns as contact (n=6), flame (n=14), and scald (n=31). The anatomical distributions were the face (n=25 vs. 29), torso (n=27 vs. 27), upper extremities (n=33 vs. 33), and lower extremities (n=34 vs. 33) for the bFGF-treated group vs. the non-bFGF–treated group, respectively. As some patients suffered burns at more than one anatomical location, there were 119 vs. 122 locations in bFGF-treated vs. non-bFGF–treated groups, respectively (Table 1).

Split-thickness skin grafting was required in some wounds for wound coverage. However, these locations were distant from the evaluation locations and excluded for further clinical and objective analyses. For the bFGF-treated group, initial use started at 2.2 ± 0.9 days (1–4 days, mean 2.0 days) and there were no other factor differences between the two groups other than the use or nonuse of a bFGF spray on the burn wounds. The bFGF was applied on day 1 as much as possible. However, because of careful clinical observation for the first 24 hours after the burn, especially handling of blister formation, the bFGF was started on day 2 and after. When a blister was formed after 24 hours, gentle management with removal of the internal fluid through minimal nicking and bFGF was applied for the bFGF-treated group.

bFGF (Trafermin, Fiblast Spray®) and non-bFGF treatment

Genetically recombinant bFGF (Fiblast Spray®, Kaken Pharmaceutical Co., Ltd., Tokyo, Japan) was used for spraying. The beginning of bFGF use varied from 2 to 4 days postburn injury. The concentration of bFGF was 30 μg of bFGF per 30 cm^2 area as 100 μg of freeze-dried bFGF dissolved in 1 mL of benzalkonium chloride solution, with 300 μL sprayed over a 30 cm^2 area from a 5 cm

distance, and 0.3 mL of this concentration solution was applied by this method. Ointment-impregnated gauze was applied to wounds treated with bFGF after waiting for 30 seconds. The bFGF administration continued until the wound had healed.

The non-bFGF treatment groups received only ointment-impregnated gauze without bFGF spraying. Standard procedures for stabilizing the burn wounds were applied for all cases.[11]

Scar scaling

Burns were evaluated by the senior authors (S. A., K. A., and T. I.), who evaluated others' patients in a blind fashion 1 year after complete wound healing. Scar scaling was determined using the Vancouver scar scale, which included pigmentation (0=normal, 1=hypo-pigmented, 2=mixed, 3=hyperpigmented), pliability (0=normal, 1=supple, 2=yielding, 3=firm, 4=ropes, 5=contracture), height (0=flat, 1= < 2 mm, 2=2–5 mm, 3 ≥5 mm), and vascularity (0=normal, 1=pink, 2=red, 3=purple).[12] Evaluation was confirmed by the other two authors, who are also burn specialists; therefore, each wound was assessed by four different evaluators. Parameters for each scar were obtained by averaging the individual score by four observers.

Cutometer

A Cutometer® MPA 580 (Courage+Khazaka electronic GmbH, Cologne, Germany) was used to evaluate skin elasticity parameters at 1 year after complete wound healing. The Cutometer is able to measure vertical deformation of the skin by suctioning into a round probe, 6 mm in diameter. A vacuum load of 500 mbar was used over the skin (or scar) surface for 1 second, followed by normal pressure for 1 second. Each measurement was repeated three times and the mean value of four adjacent points at least 6 mm apart and 12 mm from the intact skin was assessed at 25 °C room temperature and 50% humidity with air conditioning. As discussed and reported previously, two parameters of the Cutometer were used in this investigation. The Uf (depicted as R0) stands for the maximal skin (or scar) extension of the deformation at the end of the vacuum period; Ur/Uf (R7) stands for the ratio of the retraction (Ur) to the maximal extension (Uf) and reflects the elasticity of the measuring subjects.[13,14]

Durometer

The durometer used in this investigation was a TECLOCK GS-701N (Teclock Co. Ltd., Nagano, Japan), which follows the international standard of SRIS 0101 and is defined as a spring instrument to measure hardness, with a 5-mm-diameter round noninvasive gauge head, and a value range from 519 to 8379 mN (55–855 gf) at 1 year after complete wound healing. The measurement of each point was always perpendicular to the scars and was repeated five times immediately after touching the scar and at 30 seconds after touching, and the mean value of three adjacent points at least 6 mm apart and 12 mm from the edge of intact skin was assessed at 25 °C room temperature and 50% humidity with air conditioning, following the manufacturer's instructions. Informed consent was obtained from all patients and there were no complications or complaints due to durometer measurements. As a normal control, the skin hardness of similar-aged volunteers was investigated at similar anatomical and location points as a normal standard of measurement.

Moisture meter

A moisture meter (ASA-M2, Asahi Biomed Co. Ltd., Yokohama, Japan) was used to detect transepidermal water loss (TEWL), water level, and the thickness of the corneal keratinocyte layer of the skin, as well as the effective contact coefficient, determined by electrolytes in the corneal layer at 1 year after complete wound healing. The meter records were used to analyze the susceptibility of conductance using a low-frequency (160 Hz) alternate current and to detect conductance using a high-frequency (143 KHz) alternate current. The proposed formula is as follows:

$$\text{Skin conductance } (\mu c) = \text{effective contact coefficient } (\%) \times \text{water level } (\mu S).$$

To enable the use of all these formulary factors, both low- and high-frequency electric voltages were applied. The round probe of the hand-piece is 5 mm in diameter and detection was set 5 seconds after probe contact with the subject to stabilize electrodes and the skin condition. Each contact point was always perpendicular to the subject and was repeated five times, and the mean value of adjacent points at least 10 mm apart and 20 mm from the intact edge was assessed at 25 °C and 50% humidity with air conditioning, following the manufacturer's instructions. All data were immediately transferred to a personal computer for further analyses. Informed consent was obtained from all patients and there were no complications or complaints due to moisture meter measurements. The measurements were performed 1 year after compete wound healing. For moisture meter analysis, the same anatomical and location areas of bFGF-treated and non-bFGF–treated groups were compared, while skin moisture meter data of similar age-matched volunteers were investigated as a normal standard of measurement.

Statistics

The results are expressed as the mean ± standard deviation. Data between groups were evaluated by one-way analysis of variance with Bonferroni's multiple comparison procedure, and p-values < 0.05 were considered statistically significant.

RESULTS

Clinical outcome

The average healing time in the bFGF-treated and non-bFGF–treated groups was 12.0 ± 2.2 days (8–17 days) and 15.0 ± 2.7 days (11–21 days), respectively ($p < 0.01$). The scar was assessed at 1 year after complete healing.

There were 119 and 122 locations in the bFGF-treated and non-bFGF–treated groups, respectively, and postoperative HSs were clinically observed in none of 25 vs. 2 of

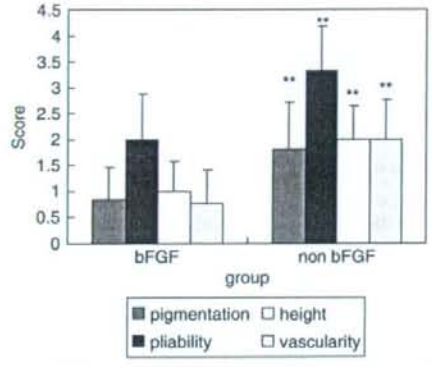

Figure 1. Vancouver scar scale. Four independent specialists evaluated at 1 year after complete wound healing. The results yielded 0.8 ± 0.6 vs. 1.8 ± 0.9, 2.0 ± 0.9 vs. 3.3 ± 0.9, 1.0 ± 0.6 vs. 2.0 ± 0.6, and 0.8 ± 0.7 vs. 2.0 ± 0.8; conventional vs. bFGF-treated, pigmentation, pliability, height, vascularity, respectively ($p < 0.01$). bFGF, basic fibroblast growth factor.

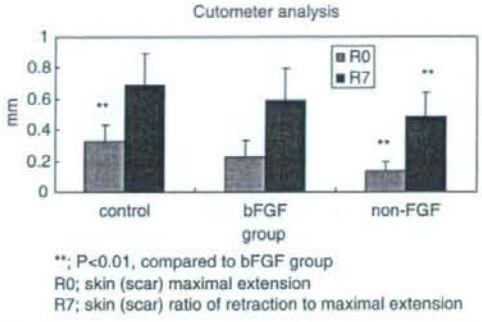

**; P<0.01, compared to bFGF group
R0; skin (scar) maximal extension
R7; skin (scar) ratio of retraction to maximal extension

Figure 2. Cutometer analysis. A Cutometer showed passive skin (scar) hardness and elasticity at 1 year after complete wound healing. The value of the maximal skin (scar) extension (denoted by R0) was significantly smaller in non-bFGF–treated scars than bFGF-treated scars and the control in the order, 0.33 ± 0.10, 0.23 ± 0.10, 0.14 ± 0.06 mm; control, bFGF-treated, non-bFGF–treated, respectively, $p < 0.01$. The skin (scar) ratio of retraction to maximal extension (denoted by R7), elasticity, was significantly smaller for non-bFGF–treated scars than bFGF-treated scars (0.69 ± 0.20, 0.59 ± 0.20, 0.49 ± 0.15 mm; control, bFGF-treated scar, non-bFGF–treated scar, respectively, $p < 0.01$). bFGF, basic fibroblast growth factor.

29 on the face, 1 of 27 vs. 3 of 27 on the torso, 1 of 33 vs. 5 of 33 on the upper extremities, and 1 of 34 vs. 4 of 33 on the lower extremities in the bFGF-treated vs. non-bFGF–treated group, respectively. The overall rate of HS formation was 2.5% for the bFGF-treated group and 11.5% for the non-bFGF–treated group. In small areas, skin grafting (< 1% of TBSA for each wound) was applied to 3 of 27 vs. 4 of 27 wounds of the torso, and 2 of 34 vs. 2 of 33 wounds on the lower extremity in the bFGF-treated and non-bFGF–treated groups, respectively. However, no HSs were observed in any location of either group at 1 year after complete wound healing and no evaluation was attempted over resurfaced scars after skin grafting.

Clinical evaluation of pigmentation, pliability, height, and vascularity showed significant differences between bFGF-treated and non-bFGF–treated scars (0.8 ± 0.6 vs. 1.8 ± 0.9, 2.0 ± 0.9 vs. 3.3 ± 0.9, 1.0 ± 0.6 vs. 2.0 ± 0.6, 0.8 ± 0.7 vs. 2.0 ± 0.8; conventional vs. bFGF-treated, pigmentation, pliability, height, vascularity, respectively, $p < 0.01$) (Figure 1). Detailed analysis of each burn location in the two groups did not show significant differences on the Vancouver scale parameter.

The bFGF was clinically permitted for use in Japan from 2001.

Skin or scar analysis by Cutometer

The values representing skin extension as R0 were significantly greater in control, nonwounded skin, followed by bFGF-treated scar, and the lowest in the non-bFGF–treated scar (0.33 ± 0.10, 0.23 ± 0.10, 0.14 ± 0.06 mm; control, bFGF-treated scar, non-bFGF–treated scar, respectively, $p < 0.01$). The relative retraction of extension, elasticity, depicted as R7, was also significantly greater in the control, followed by the bFGF-treated scar, and the lowest in the non-bFGF–treated scar (0.69 ± 0.20, 0.59 ± 0.20, 0.49 ± 0.15 mm; control, bFGF-treated scar, non-bFGF–treated scar, respectively, $p < 0.01$) (Figure 2).

Skin or scar hardness by durometer

Skin hardness measured using a durometer showed significant differences among groups. The relative value of the actual durometer reading was the lowest in the control group, which is nonwounded skin. The bFGF-treated scar was the next lowest and the non-bFGF–treated scar showed the highest value (8.0 ± 1.8, 16.2 ± 3.8, 29.3 ± 5.1; control, bFGF, non-bFGF, respectively, $p < 0.01$) (Figure 3).

Skin or scar moisture analysis

For moisture meter analyses, the effective contact coefficient was significantly higher than the nonwounded skin value (control) in both bFGF and non-bFGF–treated groups, and there was a significant difference between bFGF-treated and non-bFGF–treated groups ($10.9 \pm 1.5\%$, $18.5 \pm 1.8\%$, $4.8 \pm 1.3\%$; bFGF, non-bFGF, and nonwounded skin (control) groups, respectively, $p < 0.01$). TEWL in the bFGF-treated group was significantly less than that in the non-bFGF group (12.9 ± 2.0, $22.1 \pm 3.5\,g/m^2/hours$; bFGF-treated scar, non-bFGF–treated scar, respectively, $p < 0.01$). The bFGF-treated group showed a significantly higher TEWL value than the control (12.9 ± 2.0, $6.2 \pm 1.2\,g/m^2/hours$; bFGF-treated scar, control, respectively, $p < 0.01$). The correlation between the effective contact coefficient and

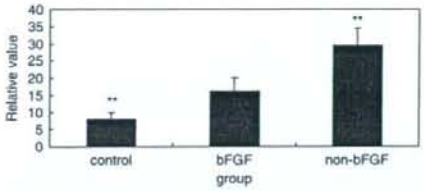

Figure 3. Durometer analysis. Direct skin (scar) hardness was obtained using a durometer at 1 year after complete wound healing. The relative value of the actual durometer reading was the lowest in the control group, which is nonwounded skin. The bFGF-treated scar was the next lowest and the non-bFGF–treated scar demonstrated the highest value (8.0 ± 1.8, 16.2 ± 3.8, 29.3 ± 5.1; control, bFGF, non-bFGF, respectively, $p < 0.01$). bFGF, basic fibroblast growth factor.

TEWL showed a significant correlation between the two ($y=0.75x+1.19$, $r^2=0.89$, $p < 0.01$).

The water content in the non-bFGF group was significantly greater than in bFGF-treated and control groups, while there was no significant difference between bFGF-treated and control groups (24.7 ± 4.5, 44.8 ± 4.9, $23.7 \pm 4.3\,\mu S$; bFGF-treated, non-bFGF–treated, control groups, respectively, $p < 0.01$; between control and non-bFGF–treated groups and between bFGF-treated and non-bFGF–treated groups). The thickness of the non-bFGF–treated group was significantly greater than both the control and the bFGF-treated groups (11.9 ± 3.0, 17.9 ± 1.7, $10.2 \pm 1.5\,\mu m$; bFGF-treated, non-bFGF–treated, control groups, respectively, $p < 0.01$; between control and non-bFGF–treated groups and between bFGF-treated and non-bFGF–treated groups) (Figure 4).

Anatomical locations of the moisture meter and the measurement conditions were similar among the three groups.

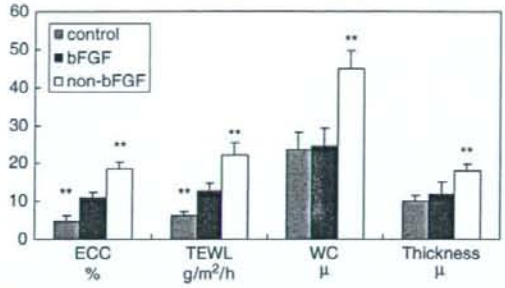

Figure 4. Moisture meter analysis. A moisture meter was used at 1 year after complete wound healing. The effective contact coefficient was significantly higher than the nonwounded skin value (control) in both bFGF-treated and non-bFGF–treated groups, and there was a significant difference between bFGF-treated and non-bFGF–treated groups ($10.9 \pm 1.5\%$, $18.5 \pm 1.8\%$, $4.8 \pm 1.3\%$; bFGF, non-bFGF, and nonwounded skin [control] groups, respectively, $p < 0.01$). Transepidermal water loss (TEWL) in control and bFGF-treated groups was significantly less than in the non-bFGF group (6.2 ± 1.2, 12.9 ± 2.0, $22.1 \pm 3.5\,g/m^2/hours$; control, bFGF-treated scar, non-bFGF–treated scar, respectively, $p < 0.01$). The water content in the non-bFGF group was significantly greater than in the bFGF-treated and control groups, while there was no significant difference between bFGF-treated and control groups (24.7 ± 4.5, 44.8 ± 4.9, $23.7 \pm 4.3\,\mu S$; bFGF-treated, non-bFGF–treated, control groups, respectively, $p < 0.01$; between control and non-bFGF–treated groups and between bFGF-treated and non-bFGF–treated groups). The thickness of the non-bFGF–treated group was significantly greater than both the control and the bFGF-treated groups (11.9 ± 3.0, 17.9 ± 1.7, $10.2 \pm 1.5\,\mu m$; bFGF-treated, non-bFGF–treated, control groups, respectively, $p < 0.01$; between control and non-bFGF–treated groups and between bFGF-treated and non-bFGF–treated groups). bFGF, basic fibroblast growth factor.

DISCUSSION

Fibroblast growth factors (FGFs) play important roles in tissue repair. Among FGFs, FGF-2 or bFGF contributes to reepithelialization and collagen deposition in a "knock-out" mouse model. Further, bFGF is also involved in neuronal protection and repairs ischemic, metabolic, or traumatic brain injury.[15]

Pretreatment evaluation of second-degree burns or the depth of dermal injuries is sometimes a clinical concern[16]; however, mostly deep dermal burns in this investigation were included, as diagnosed by four burn and scar specialists, and the clinical course followed; although more precise, easy, and objective assessment methods may be further required for generalizing deep dermal "second-degree" burns using a reproducible method.[17,18]

Our therapeutic regimens of bFGF treatment for the second-degree burns in this investigation started as early as on arrival day of postburn, and burn wound healing was completed at 12 days for the bFGF-treated group; this may be compatible with the endogenous bFGF expressions observed during day 4 to day 11 as observed in rats immunohistochemically.[8]

Burn-wounded human skin obtained 2–4 weeks after wounding showed FGF receptor (FGFR)-1 and -3 expressions in basal and supra-basal layers of the epidermis as well as granulation tissues such as neo-capillaries, fibroblasts/myofibroblasts, and inflammatory cells. Thus, the bFGF and its receptor signaling pathway as well as bFGF expressed in the dermal extracellular matrix may contribute to promoting reepithelialization during the wound-healing process.[19]

The quality of the scar or the quality of wound healing should be determined after the completion of wound healing.

Clinical multiple-investigator evaluations of burn scars in the bFGF-treated group by the Vancouver scar scale were significantly improved in all parameters compared with non-bFGF–treated scars. The ratio of each parameter of pigmentation, pliability, height, and vascularity was 1:2.25, 1.165, 1:2, and 1:2.5: bFGF-treated scar:non-bFGF–treated scar, respectively. These data were comparable to pediatric second-degree burn scars, which were 1:2.43, 1:2.18, 1.6, and 1:2.38: bFGF-treated:non-bFGF–treated, respectively.[20] Previous use of a durometer

for scar hardness in post–split-thickness skin grafting showed significant improvement in association with clinical skin hardness.[21] In this investigation, another objective tool of scar quality, a Cutometer, used for passive scar extension and relative retraction to the extended scar, which reflects the elasticity of the scar, showed significant improvement in bFGF-treated second-degree, most deep dermal, burns.

Additional studies using a moisture meter enabled the evaluation of corneal layer (stratum corneum) functions by the effective contact coefficient, together with TEWL, water content, and layer thickness. Abnormal functioning of corneal layers is well demonstrated in atopic dry skin studies by increased TEWL, decreased water content, and increased thickness as seen in atopic dry skin, which is thickened. As atopic skin decreases the amount of intercellular phospholipids or ceramides, this may account for the damaged function of the corneal layers.[22]

The epidermis regulates the collagen I synthesis by dermal fibroblasts and bFGF and insulin-like growth factor increased collagen production by increasing the fibroblast cell number both in monoculture and in coculture with keratinocytes.[23] In wounded skin, especially deeper wounds, HSs and keloids showed high TEWL and water content values. These data also suggest that proliferative changes in the dermis may affect the corneal layers. As one possible mechanism, especially in keloids and HSs, complex epithelial–mesenchymal interactions may modulate transforming growth factor-β (TGF-β), which may be one of the core pathogenic factors for keloids, and keloid-derived keratinocytes highly activated TGF-β expression levels in a paracrine fashion.[24]

TGF-β is expressed in the experimental burn model, although the expression pattern fluctuated during the first 15 days after the deep dermal burn as well as other cytokines such as bFGF, IL-1, and nerve growth factor (NGF).[25]

In rats, liposomal gene transfer of keratinocyte growth factor improved wound healing and altered local immunohistochemical expression by decreasing TGF-β but by increasing FGF expression at the wound edge and under the wound bed, although the burn type was extensive with TBSA 30% and third degree.[26] This suggests that local bFGF may change the TGF-β expression pattern and thus may not lead to excessive collagen deposition as observed in HSs or keloids under certain conditions.

The bFGF-treated scars may have a better process of skin remodeling, which may avoid the subsequent development of fibro-proliferative disorders.[27] As the frequency of tape-stripping increases, water-holding defects of the corneal layers (stratum corneum) are associated with a higher value of TEWL.[28] Thus, TEWL is an important marker of hydration for epithelialization or re-epithelialization after healing. The effective contact coefficient is affected by skin surface electrolytes such as sweating; however, this value also reflects the barrier function of the skin. In our study, there was a correlation between the effective contact coefficient and TEWL. The thickness of both control nonwounded skin and bFGF-treated scars was significantly less than non-bFGF scars.

The use of bFGF for second-degree burns accelerates wound healing and improves the quality of scars by objective measurement of scar quality as well as multiple-investigator subjective evaluations.

ACKNOWLEDGMENTS

This study was supported by grants from the Japanese Ministry of Education, Sports and Culture, #18390478, 18591967, 18659526, and 19406029.

REFERENCES

1. Engrav LH, Heimbach DM, Reus JL, Harnar TJ, Marvin JA. Early excision and grafting vs. non-operative treatment of burns of interminant depth: a randomized prospective study. *J Trauma* 1983; 23: 1001–4.
2. Muangman P, Deubner H, Honari S, Heimbach DM, Engrav LH, Klein MB, Gibran NS. Correlation of clinical outcome of integra application with microbiologic and pathological biopsies. *J Trauma* 2006; 61: 1212–7.
3. Monstrey S, Hoeksema H, Saelens H, Depuydt K, Hamdi M, Van Landuyt K, Blondeel P. A conservative approach for deep dermal burn wounds using polarized-light therapy. *Br J Plast Surg* 2002; 55: 420–6.
4. Herndon DN, Hawkins HK, Nguyen TT, Pierre E, Cox R, Barrow RE. Characterization of growth hormone enhanced donor site healing in patients with large cutaneous burns. *Ann Surg* 1995; 221: 649–56.
5. Ravage ZB, Gomez HF, Czermak BJ, Watkins SA, Till GO. Mediators of microvascular injury in dermal burn wounds. *Inflammation* 1998; 22: 619–29.
6. Iwashita N, Muramatsu H, Toriyama K, Torii S, Muramatsu T. Expression of midkine in normal and burn sites of rat skin. *Burns* 1999; 25: 119–24.
7. Galeano M, Altavilla D, Bitto A, Minutoli L, Calò M, Lo Cascio P, Polito F, Giugliano G, Squadrito G, Mioni C, Giuliani D, Venuti FS, Squadrito F. Recombinant human erythropoietin improves angiogenesis and wound healing in experimental burn wounds. *Crit Care Med* 2006; 34: 1139–46.
8. Kibe Y, Takenaka H, Kishimoto S. Spatial and temporal expression of basic fibroblast growth factor protein during wound healing of rat skin. *Br J Dermatol* 2000; 143: 720–7.
9. Gibran NS, Isik FF, Heimbach DM, Gordon D. Basic fibroblast growth factor in the early human burn wound. *J Surg Res* 1994; 56: 226–34.
10. Fu X, Shen Z, Chen Y, Xie J, Guo Z, Zhang M, Sheng Z. Randomised placebo-controlled trial of use of topical recombinant bovine basic fibroblast growth factor for second-degree burns. *Lancet* 1998; 352: 1661–4.
11. Fujii T. Local treatment for extensive deep dermal thickness burn and follow-up study. *Acta Chir Plast* 1990; 32: 46–56.
12. Baryza MJ, Baryza GA. The Vancouver scar scale: an administration tool and its interrater reliability. *J Burn Care Rehabil* 1995; 16: 535–8.
13. Draaijers LJ, Botman YA, Tempelman FR, Kreis RW, Middelkoop E, van Zuijlen PP. Skin elasticity meter or subjective evaluation in scars: a reliability assessment. *Burns* 2004; 30: 109–14.
14. Morita A, Kobayashi K, Isomura I, Tsuji T, Krutmann J. Ultraviolet A1 (340–400 nm) phototherapy for scleroderma in systemic sclerosis. *J Am Acad Dermatol* 2000; 43: 670–4.

15. Steiling H, Werner S. Fibroblast growth factors: key players in epithelial morphogenesis, repair and cytoprotection. *Curr Opin Biotechnol* 2003; 14: 533–7.
16. Dunkin CS, Pleat JM, Gillespie PH, Tyler MP, Roberts AH, McGrouther DA. Scarring occurs at a critical depth of skin injury: precise measurement in a graduated dermal scratch in human volunteers. *Plast Reconstr Surg* 2007; 119: 1722–32.
17. Sheridan RL, Schomaker KT, Lucchina LC, Hurley J, Yin LM, Tompkins RG, Jerath M, Torri A, Greaves KW, Bua DP. Burn depth estimation by use of indocyanine green fluorescence: initial human trial. *J Burn Care Rehabil* 1995; 16: 602–4.
18. Pape SA, Skouras CA, Byrne PO. An audit of the use of laser Doppler imaging (LDI) in the assessment of burns of intermediate depth. *Burns* 2001; 27: 233–9.
19. Takenaka H, Yasuno H, Kishimoto S. Immunolocalization of fibroblast growth factor receptors in normal and wounded human skin. *Arch Dermatol Res* 2002; 294: 331–8.
20. Akita S, Akino K, Imaizumi T, Tanaka K, Anraku K, Yano H, Hirano A. The quality of pediatric burn scars is improved by early administration of basic fibroblast growth factor. *J Burn Care Res* 2006; 27: 333–8.
21. Akita S, Akino K, Imaizumi T, Hirano A. A basic fibroblast growth factor improved the quality of skin grafting in burn patients. *Burns* 2005; 31: 855–8.
22. Imokawa G, Abe A, Jin K, Higaki Y, Kawashima M, Hidano A. Decrease level of ceramides in stratum corneum of atopic dermatitis. *J Invest Dermatol* 1991; 96: 523–6.
23. Harrison CA, Gossiel F, Bullock AJ, Sun T, Blumsohn A, MacNeil S. Investigation of kertinocyte regulation of collagen I synthesis by dermal fibroblasts in a simple in vitro model. *Br J Dermatol* 2006; 154: 401–10.
24. Suetake T, Sasai S, Zhen YX, Ohi T, Tagami H. Functional analyses of the stratum corneum in scars. Sequential studies after injury and comparison among keloids, hypertrophic scars, and atrophic scars. *Arch Dermatol* 1996; 132: 1453–8.
25. Jurjus A, Atiyeh BS, Abdallah IM, Jurjus RA, Hayek SN, Jaoude MA, Gerges A, Tohme RA. Pharmacological modulation of wound healing in experimental burns. *Burns* 2007; 33: 892–907.
26. Pereira CT, Herndon DN, Rocker R, Jeschke MG. Liposomal gene transfer of keratinocyte growth factor improves wound healing by altering growth factor and collagen expression. *J Surg Res* 2007; 139: 222–8.
27. Rahban SR, Garner WL. Fibroproliferative scars. *Clin Plast Surg* 2003; 30: 77–89.
28. Tagami H, Yoshikuni K. Interrelationship between water-barrier and reservoir functions of pathologic stratum corneum. *Arch Dermatol* 1985; 121: 642–5.

<第2回瘢痕・ケロイド治療研究会ランチョンセミナー>

創傷治癒における瘢痕期の柔軟性，硬度，カラーマッチ，角質機能改善に貢献するbFGF製剤

長崎大学大学院医歯薬学総合研究科形成外科

秋田定伯

Improvement of color matching in cases of bFGF and split-thickness skin grafting using a colorimeter

Sadanori Akita

Department of Plastic and Reconstructive Surgery, Nagasaki University, Graduate School of Biomedical and Sciences, Nagasaki, Japan

Pigmentation is sometimes a major concern for patients undertaking surgery. Color differences between the normal skin and grafted or flap-transferred skin are not objectively evaluated. Here, an easy and light colorimeter analysis was performed for flap surgery and skin grafting with basic fibroblast growth factor (bFGF) over the grafted wound beds. bFGF produces softer and high quality surface barriers, and also improved scar clarity, redness, and yellow-color scores. Earlier use of bFGF with skin grafting leads to better color matching to normal, undamaged skin.

はじめに

“創”の評価は硬度から上皮の機能にまで多岐にわたる。色素沈着した皮膚は植皮術(分層または全層)，皮弁術(遊離皮弁または局所皮弁)では患者の最も重要な“訴え”となることがある。メラノサイトからのメラノソームの伝授機構が判明しつつある[1]ものの，臨床的な客観的な観察は少ない。簡易型色素解析器を用いて簡易で客観的な臨床検討を行った。

対象と方法

創傷治癒後1年以上の瘢痕の色素状態を，①皮弁の選択による違い，②分層植皮時の併用療法の違いにより，臨床例で検討した。使用した色素計は，簡易色素分析器(NF-333，日本電色工業社製)であり，本体440 g，接触子110 gと軽量であり，データはL，a，bのパラメータで分光解析され，データは直接，表計算ソフトウェアのエクセル(Microsoft社)へ転送可能である。

結　果

1. 皮弁術での評価

乳房再建時の術後の色調を広背筋皮弁群と腹直筋皮弁群で比較検討した。平均年齢45.3±15.2歳で有茎広背筋による再建が3例，有茎腹直筋皮弁による再建が5例の合計8例であった。術後経過時間は平均4.7±2.8年(最小1年，最大6年)であった。全例で移植後の皮弁生着に問題はなく完全生着であった。簡易色素

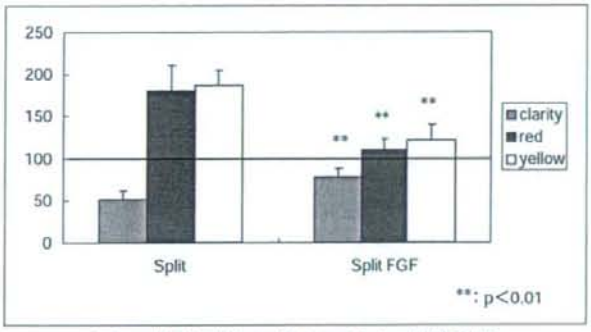

図 1. 簡易色素計での各々のパラメータ解析結果
各々のパラメータは bFGF を用いた分層植皮群が正常対照に近似した(100)値となっている。分層植皮術単独では，明瞭度は低く，赤色，黄色は強い結果となり，臨床的な色素沈着を反映すると考えられた。

計計測では，明瞭度(L, Clarity)が広背筋皮弁で 56.5±11.6，赤色(a)が 170.1±31.6，黄色(b)が 164.7±21.6 であった(正常対照部位を 100 としての相対値)。一方，腹直筋皮弁では，各々 85.7±13.2，82.5±11.1，86.9±14.0 と各々のパラメータでは腹直筋弁において有意に正常対照と近似していた($p<0.01$)。

2. 分層植皮術での評価

大腿外側からの分層植皮術(10/1,000 インチ，電動デルマトームによる)の際に瘢痕の質を改善する目的[2]で bFGF 製剤の噴霧を行った瘢痕(13 例と 8 例，平均 3.8±1.9 年と平均 3.5±1.6 年の術後での評価)を簡易色素計にて計測すると，分層植皮のみ，bFGF 併用の明瞭度(L)，赤色(a)，黄色(b)は 51.0±10.4 vs. 78.1±9.6，180.3±30.8 vs. 109.6±13.0，187.2±17.6 vs. 121.1±18.7($p<0.01$)であり各々のパラメータ毎に bFGF 使用により正常の皮膚に近い色調を示した(図 1)。

まとめ

皮弁術では，ドナー部位の違いにより，色素計では特に赤色，黄色の色調で異なっていた。分層植皮術時に bFGF を用いると，明瞭度，赤色，黄色のパラメータ全般に正常域に近似していた。これまでの報告では，bFGF 製剤の創傷への投与で，瘢痕硬度が低下し[2]，臨床解析と共に，角質水分計での解析でも改善していたが[3][4]，今回の結果から，色調の改善にも貢献することがわかった。

参考文献

1) Kuroda, T. S., Fukuda, M. : Rab27 A-binding protein Slp2-a is required for peripheral melanosome distribution and elongated cell shape in melanocytes. Nat Cell Biol. 12 : 1195-1203, 2004.
2) Akita, S., Akino, K., Imaizumi, T., Hirano, A. : A basic fibroblast growth factor improved the quality of skin grafting in burn patients. Burns. 31 : 855-858, 2005.
3) Akita, S., Akino, K., Imaizumi, T., Tanaka, K., Anraku, K., Yano, H., Hirano, A. : The quality of pediatric burn scars is improved by early administration of basic fibroblast growth factor. J Burn Care Res(formerly J Burn Care Rehabil). 27 : 333-338, 2006.
4) Akita, S., Akino, K., Tanaka, K., Anraku, K., Hirano, A. : A basic fibroblast growth factor improves lower extremity wound healing with a porcine-derived skin substitute. J Trauma. in press.

Report

Human mesenchymal stem cells may be involved in keloid pathogenesis

Kozo Akino[1], MD, PhD, Sadanori Akita[2], MD, PhD, Aya Yakabe[2], MD, Takao Mineda[3], PhD, Tomayoshi Hayashi[4], MD, PhD, and Akiyoshi Hirano[2], MD

From the [1]Division of Anatomy and Neurobiology, [2]Division of Plastic and Reconstructive Surgery, [3]Division of Oral Cytology and Cell Biology, and [4]Department of Pathology, Nagasaki University, Nagasaki, Japan

Correspondence
Sadanori Akita, MD, PhD
Division of Plastic and Reconstructive Surgery
Department of Developmental and Reconstructive Medicine
Graduate School of Biomedical and Sciences
Nagasaki University
1-7-1 Sakamoto
Nagasaki 852 8501
Japan
E-mail: akitas@hf.rim.or.jp

Abstract

Background The pathogenesis of keloid is poorly understood. Although vigorous investigations have attempted to elucidate the mechanisms or causative factors of keloid, there are little data on why keloids are very intractable and recur easily in each patient.

Methods In an attempt to analyze the possible interaction between human mesenchymal stem cells and keloid-derived fibroblasts, the dual-chamber cell-migration assay, cell proliferation, ultrastructural morphology, and Western blot analysis were used to investigate the production of the extracellular matrices of the coculture.

Results Cell proliferation was not significantly different between keloid-derived fibroblasts and normal dermal fibroblasts during a 4-day observation period. There was a significant cell migration of human mesenchymal stem cells when keloid-derived fibroblasts were placed in the bottom chamber, compared to when normal dermal fibroblasts were placed in the same way in 8-μm diameter pore membranes (190.6 ± 51.45 and 32.0 ± 6.20 cells/field, respectively, $P < 0.01$). With 3-μm diameter pores, the human mesenchymal stem cells migrated in the pores only when the keloid-derived fibroblasts were placed in the bottom chambers (6.4 ± 3.84 cells/field). Monolayer coculture of human mesenchymal stem cells and keloid-derived fibroblasts demonstrated further functional differentiation, such as collagen secretion and abundant rough endoplasmic reticulum. Western blot analysis of the cells in the modified dual-chamber culture demonstrated most significantly abundant fibronectin expression when the human mesenchymal stem cells contained keloid fibroblasts.

Conclusion The results of this study may indicate that human mesenchymal stem cells participate and recruit in keloid pathogenesis by differentiating themselves toward keloid recalcitrant formation and progression.

Introduction

Despite extensive research focused on keloid mechanisms and treatment including the possible involvement of fibrogenic factors, such as transforming growth factor-β (TGF-β),[1] insulin-like growth factor-1 (IGF-1),[2] and platelet-derived growth factor (PDGF),[3] as well as defects in fibrin degradation represented by plasminogen activator inhibitor-1 (PAI-1),[4] little is known on which cell types play a crucial role in the pathogenesis of keloids. While keloid scars recur in individual patients in the same area, some patients develop keloid scars in multiple areas after very minor trauma. Keloid scars are recalcitrant to medical, therapeutic-radiation, or surgical treatments, and they even voluntarily extend over the original wound boundary. There is no fundamental treatment for keloid scars, and the current treatment is by palliative modalities, such as pressure, anti-allergic medication, or steroid injection.[5] Recent developments in stem cell biology have led to the potential application of regenerative medicine by stem cells in the wound-healing process. Among the somatic stem cells, the human bone marrow–derived mesenchymal stem cells (hMSC) are well characterized by surface markers, cell proliferation, differentiation, and regulation.[6] Lipid mediators, such as cysteinyl leukotrienes, are involved in human mesenchymal stem cell differentiation.[7] Keloid fibroblasts significantly enhance the extracellular matrix expression, such as collagen type 1, fibronectin, and PAI-1, under TGF-β and IGF-1 in a dose-dependent manner.[8] Thus, excessive extracellular matrix production from keloid fibroblast is targeted by therapy and pathogenesis. In a mouse model of systemic sclerosis by daily injection of bleomycin, sclerotic cutaneous change was reversed through intravenous administration of antibody against TGF-β[9]; however, detailed information concerning the regulation of

International Journal of Dermatology 2008, 47, 1112–1117

influx suppression of granulocytes such as mast cells and eosinophils is still unknown. Moreover, systemically administered mesenchymal stem cells, which are able to reverse bleomycin-induced fibrotic effects in the lung tissue,[10] are a possible therapeutic modality. The interaction between keloid-derived fibroblasts and mesenchymal stem cells has therefore been investigated for cell ultrastructure as well as cell proliferation, cell migration, and extracellular matrix production.

Materials and Methods

Human mesenchymal stem cells

Human mesenchymal stem cells from a single human bone marrow donor were isolated by density gradient centrifugation and strictly sorted as positive for markers such as CD105, CD166, CD29, and CD44, and negative for cell surface makers such as CD14, CD34, and CD45. Human mesenchymal stem cells were purchased from BioWhittaker Inc. (cat. no. PT-2501, Walkersville, MD) and the cryopreserved cells were thawed immediately according to the manufacturer's instructions. Two different donor-derived hMSCs, obtained from two Asian men (23 and 24 years old), were used for this study.

The cells were cultured in "basic medium" of Dulbecco's modified Eagle's medium (DMEM) containing low glucose supplemented with 10% fetal bovine serum (FBS, heat-inactivated, cat. no. 16000-044, Gibco, Invitrogen Life Technologies, Tokyo, Japan), 200 mM L-glutamine, and penicillin (100 U/mL) and streptomycin (100 μg/mL) at 37 °C in 95% humidified air and 5% CO_2. The medium was changed every 3 days until the cells were confluent, and they were then passaged up to three times. The growth characteristics during the four passages in FBS were indistinguishable. The cells were washed using 10 mL of phosphate-buffered saline (PBS) and then liberated by exposure to 0.25% trypsin/1 mM EDTA (Gibco, cat. no. 25200-056) for 3 min at 37 °C, followed by tapping of the dishes and the addition of 5 mL of culture medium. The cells were centrifuged at 400 ***g***, and then resuspended in basic medium for the following *in vitro* examinations. The other cells were stored at −70 °C until use in a solution containing 5% human serum albumin (IS Japan Co., Ltd, Saitama, Japan, cat. no. 9988) and 10% dimethylsulfoxide (Sigma-Aldrich, Tokyo, Japan, cat. no. 41641) according to the manufacturer's instructions.

Keloid-derived fibroblasts and normal dermal fibroblasts

Three different human keloid samples were used in this investigation, taken from three different Japanese male patients (17, 21 and 23 years old) after surgical excision and subsequent adjuvant electron radiation therapy. Informed consent was obtained from each patient. The tissues were divided for tissue samples and cell culture. Some tissues were fixed in ice-cold 4% paraformaldehyde solution for 3 days, embedded in paraffin, and cut into 5-μm thick sections, and some were prepared for ultra-structural analysis. Slides were stained with hematoxylin and eosin, and Toluidine blue. For cell culture, tissue excised from a keloid lesion was minced and placed on 100-mm culture plates, consisting of the same basic medium as hMSCs at 37 °C in 95% humidified air and 5% CO_2 as previously established.[2] Normally, keloid-derived fibroblasts can be observed under a phase-contrast microscope after a 2-week culture with 3-day medium change. The cells were passaged when 70–80% confluence was reached. Up to five passages from initial cell dissemination were used in this experiment.

As a control, normal human dermal fibroblasts (CCS-2511), which were obtained from two Asian men (19 and 21 years old), were cultured using an FGM Bullet kit (CCM-3130; Takara Bio Inc., Shiga, Japan), containing 500 mL of fibroblast basal medium supplemented with hFGF-2, insulin, FBS, and gentamicin/amphotericin-B (manufactured by Cambrex Corp., East Rutherford, NJ, and distributed by Asahi Technoglass Corp., Tokyo, Japan), on 100-mm culture plates at 37 °C in 95% humidified air and 5% CO_2. After 24-h incubation, the growth medium was changed to basic medium in accordance with hMSCs and keloid-derived fibroblasts. The growth medium was changed every other day until the cells were confluent, and they were then passaged up to three times. The cells were washed using 10 mL of PBS and then liberated by exposure to 0.25% trypsin/1 mM EDTA (Gibco) for 3 min at 37 °C, followed by tapping of the dishes and the addition of 5 mL of culture medium. The cells were centrifuged at 400 ***g***, and then resuspended in basic medium for the following experiments. The other cells were stored at −70 °C until used in a solution containing 5% human serum albumin (IS Japan, Co., Ltd) and 10% dimethylsulfoxide (Sigma-Aldrich) according to the manufacturer's instructions.

Cell proliferation

Cell proliferation for keloid-derived fibroblasts and normal dermal cells was determined as previously established.[11] In short, 1×10^4 cells were counted using a Beckman Coulter® Cell and Particle Counter (Beckman Coulter, Tokyo, Japan) in 24-well culture dishes after 24-h incubation in basic medium. All cells were counted in triplicate and the average value was calculated for each well. Cell death was minimal and a trypan blue cell viability assay demonstrated less than 1% nonviable cells throughout the experimental observation period in basic medium.

Dual-modified Boyden chamber cell migration assay and coculture assay

First, cell culture inserts (3.0 μm/6-well or 8.0 μm/6-well) (upper chamber) initially containing 1×10^5 hMSCs or normal dermal fibroblasts in basic medium overnight were placed on the seeded top of a 6-well plate dish (lower chamber) in the same basic medium.[12] After overnight incubation, hMSCs or normal dermal fibroblasts attached to the upper chambers were transferred onto each lower chamber, onto which each cell (human keloid-derived fibroblast cells or normal dermal fibroblasts) or medium alone (no cell) was already seeded at about 50% confluence of each 6-well

plate in basic medium. The migration activity was evaluated 16 h later by counting the number of invaded hMSCs on the reverse surfaces of 3-μm and 8-μm pore membranes, stained with Nuclear First Red (TA-060-NF) LAB Vision Corp. (Fremont, CA). The experiments were repeated in five different wells for each assay after obtaining the average values of five counts microscopically.

Some hMSCs were then used for direct coculture in basic medium for further direct analysis. In the direct coculture analysis, 1×10^5 hMSCs and 1×10^5 keloid-derived fibroblasts, or 1×10^5 hMSCs and 1×10^5 normal dermal fibroblasts were incubated for 24 h in 6-well plates and subsequently sent for electron microscopic analyses. For each group, five different cell culture plates were individually investigated.

Electron microscopy

In order to perform transmission electron microscopy, keloid tissues and basic medium containing hMSCs in 10% FBS were prefixed in half-strength Karnovsky's fixative (pH 7.2, osmolarity 1400 mOsm) buffer consisting of 2% paraformaldehyde and 2.5% glutaraldehyde in 0.1 M cacodylate buffer for 2 h, postfixed in 2% osmium tetroxide solution (pH 7.4), dehydrated using a conventional procedure and embedded in epoxy resin. The hMSCs were cultured for 4 days in basic medium of low glucose DMEM supplemented with 10% FBS and 200 mM L-glutamine, penicillin (100 U/mL) and streptomycin (100 μg/mL). The cells were first centrifuged, and then washed with PBS, and the pellets at the bottom of the tube were subsequently dissolved with fixative after washing with PBS. Embedded specimens were ultrathin-sectioned and double-stained with uranyl acetate and lead citrate. These sections were observed using a Hitachi H-7100 electron microscope (Hitachi, Tokyo, Japan) at 75 kV accelerating voltage.

Next, specimens of the cell culture insert, to which the hMSCs were attached on the reverse side, prepared for scanning electron microscopy, were dehydrated and dried by critical-point drying apparatus (HCP-2, Hitachi) for scanning electron microscopy. Specimens in a 35-mm tissue culture dish (3000-035, Iwaki, Tokyo, Japan) were dehydrated through an ethanol series and freeze-dried in t-butyl alcohol in a freeze-dryer. The dried specimens were scatter-coated with gold using an ion-coater (IB-2, Eiko Engineering, Tokyo, Japan) and observed with a scanning electron microscope (S-3500 N, Hitachi)

Western blotting

For Western blotting, extracts of 5×10^5 hMSCs and 5×10^5 keloid-derived fibroblasts, 5×10^5 hMSCs and 5×10^5 normal dermal fibroblasts, or 5×10^5 normal dermal fibroblasts and 5×10^5 keloid-derived fibroblasts, in the upper and in the lower chamber, respectively, from 8-μm pore-sized dual-chamber method, were prepared after 24-h incubation cells were lysed using celLytic-M (cat. no. C2978, Sigma-Aldrich, St. Louis, MO) with aliquots containing 20 μg as protein as measured by spectrophotometer, run on an e-pagel (ATTO Co. Ltd, Tokyo, Japan) sodium dodecyl sulfate (SDS)–polyacrylamide gel electrophoresis system (25 mM Tris, 0.1% SDS and 192 mM glycine solution). Cells for Western blotting were obtained only from each lower chamber. The gels were washed with TBST solution (20 mM Tris-HCl, pH 7.4, 0.5 M NaCl, 0.05% Tween-20) for 3 min three times in a horizontal shaker. The proteins were then transferred to Hybond-P PVDF membrane (RPN2020P, Amersham Pharmacia Biotech Inc., Piscataway, NJ) in a solution of 25 mM Tris, 20% methanol, and 192 mM glycine.

The nonspecific background was blocked with 0.2% bovine serum albumin in PBS for 1 h in a horizontal shaker. The membranes were incubated for 3 h with primary antibodies against mouse fibronectin monoclonal antibody (1 : 200 dilution, Santa Cruz Biotechnology Inc., Santa Cruz, CA, cat. no. sc-8422) or mouse monoclonal GAPDH (glyceraldehyde 3-phosphate dehydrogenase) antibody (1 : 300 dilution, Santa Cruz Biotechnology, cat. no. sc-47724), and then incubated with secondary antibodies of mouse anti-rabbit horseradish peroxidase conjugated antibody (1 : 1000 dilution; Amersham Pharmacia Biotech). The blotted membranes were washed with TBST solution after each primary or secondary antibody for 3 min three times in a horizontal shaker. After incubation with ECL Plus (Amersham Pharmacia Biotech) for 3 min, the membranes were visualized in a CCD camera-loaded chemiluminescence system for protein expression (ATTO Light Capture, cat. no. 6962). Five different samples from different tissues of each group were investigated using Western blot analyses, and the protein levels were densitometrically analyzed using a CS analyzer (ATTO). For each band, the mean of five measurements was calculated. The fibronectin expression levels were normalized against internal GAPDH expression levels of each tissue.

Statistical analysis

The cell number values are expressed as mean ± standard deviation. The data among the groups were analyzed by one-way analysis of variance followed by Scheffe's *F*-test using add-in software, Statcel, to Microsoft Excel 2000. *P*-values less than 0.05 were considered significant.

Results

Cell proliferation

The keloid-derived fibroblasts proliferated at $2.4 \pm 2.48 \times 10^4$ cells at day 1, 24 h after plating the cells, then $5.1 \pm 2.07 \times 10^4$ cells at day 2, $13.2 \pm 1.16 \times 10^4$ cells at day 3, and $11.3 \pm 1.34 \times 10^4$ cells at day 4 ($P < 0.01$).

The normal dermal fibroblasts proliferated at $3.8 \pm 1.53 \times 10^4$ cells at day 1, then $5.2 \pm 3.11 \times 10^4$ cells at day 2, $7.3 \pm 3.29 \times 10^4$ cells at day 3, and $10.7 \pm 4.58 \times 10^4$ cells at day 4 ($P < 0.01$). Both the keloid-derived fibroblasts and normal dermal fibroblasts demonstrated linear cell proliferation during the 4-day observation.

Quantitative cell migration

The hMSCs were vital and the cells were healthy throughout the experiment. When normal dermal fibroblasts were placed in the lower chambers and with 3-μm pore membranes, the hMSCs only invaded 0.4 ± 0.5 cells/field. The keloid-derived fibroblasts induced hMSC migration through 3-μm pore membranes at 6.4 ± 3.8 cells/field, while keloid-derived fibroblasts induced 2.4 ± 1.3 cells/field cell migrations of normal dermal fibroblasts. There was a significant difference in hMSC migration with 8-μm membranes. The cell migration among the hMSCs in the upper and normal fibroblasts in the lower, the hMSCs in the upper and the lower and normal dermal fibroblasts in the upper, and the keloid-derived fibroblasts in the lower were 32.0 ± 6.2, 190.6 ± 51.4, 65.2 ± 9.0 cells/field, respectively, $P < 0.01$ (Fig. 1a,b). Since the keloid-derived fibroblasts demonstrated significant cell migration, further investigation following cell–cell interaction, direct coculture between the keloid-derived fibroblasts and hMSCs, as well as keloid-derived fibroblast analysis was performed.

Electron microscopy

In the dual-cell migration assay, cell morphology in the electron microscope demonstrated the differentiation of cells, such as conspicuous nucleoli and cytoplasmic subcytomembranous fibrils with dense bodies indicating myofibroblast-like structure in some cells, and thick collagen secreted granules as well as frequent mitoses (Fig. 2). Subsequently, monolayer coculture of hMSCs and keloid-derived fibroblasts demonstrated further functional differentiation, such as collagen secretion and abundant rough endoplasmic reticulum (Fig. 3).

Western blotting and quantification of extracellular matrix

The Western blot analysis of either the hMSCs in the upper chamber or none and either normal dermal fibroblasts or keloid-derived fibroblasts in the lower chamber for 24 h demonstrated significant difference in the fibronectin expression. Normalized by internal GAPDH expression for each band, the hMSCs in the upper and normal dermal fibroblasts depicted 0.8 ± 0.2, the hMSCs in the upper and keloid-derived fibroblasts depicted 2.2 ± 0.4, and normal dermal fibroblasts in the upper and keloid-derived fibroblasts in the lower depicted 1.0 ± 0.2 relative value of fibronectin expression ($P < 0.01$, between hMSCs in the upper with normal fibroblasts in the lower and hMSCs in the upper with keloid-derived fibroblasts in the lower, and between hMSCs in the upper with keloid-derived fibroblasts in the lower and normal fibroblasts in the upper with keloid-derived fibroblasts in the lower) (Fig. 4).

Discussion

Keloid-derived fibroblasts proliferated in the basic medium of hMSCs during the 4-day observation. There was little cell apoptosis during the experimental period. The dual-chamber assay demonstrated that hMSCs significantly induced cell migration with 8-μm pore membranes when keloid-derived fibroblasts were placed in the bottom plates compared to normal dermal fibroblasts in the bottom plates. In addition, even 3-μm pores, which normally do not permit the passage of hMSCs, were able to migrate. The significant cell migration suggests that keloid-derived fibroblasts are able to induced hMSC chemoattraction toward keloid cells. Normal fibroblast failed to be chemoattracted to keloid-derived fibroblasts.

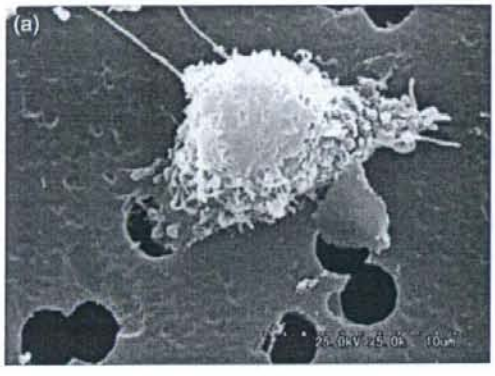

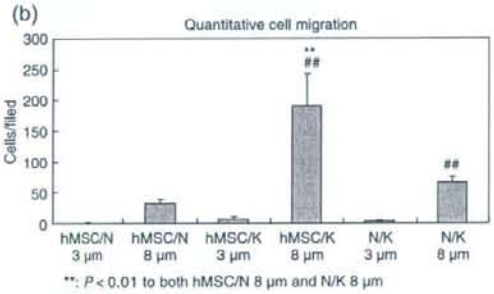

**: $P < 0.01$ to both hMSC/N 8 μm and N/K 8 μm
##: $P < 0.01$ to each 3 μm

hMSC/N: hMSCs in the upper and normal dermal fibroblasts in the lower chamber
hMSC/K: hMSCs in the upper and keloid-derived fibroblasts in the lower chamber
N/K: normal dermal fibroblasts in the upper and keloid-derived fibroblasts in the lower chamber

Figure 1 Cell migration in the reverse side of 3-μm pore membranes when keloid-derived fibroblasts were placed in the lower chamber in the dual-chamber assay. There was significant cell migration when keloid-derived fibroblasts were placed in the bottom chamber compared to when normal dermal fibroblasts ($P < 0.01$) and 8-μm pore membranes were used. hMSCs were able to pass through even 3-μm pore membranes when keloid-derived fibroblasts were used, but very few when normal dermal fibroblasts were used. More than 10-μm-diameter hMSCs were able to pass through the 3-μm diameter pores

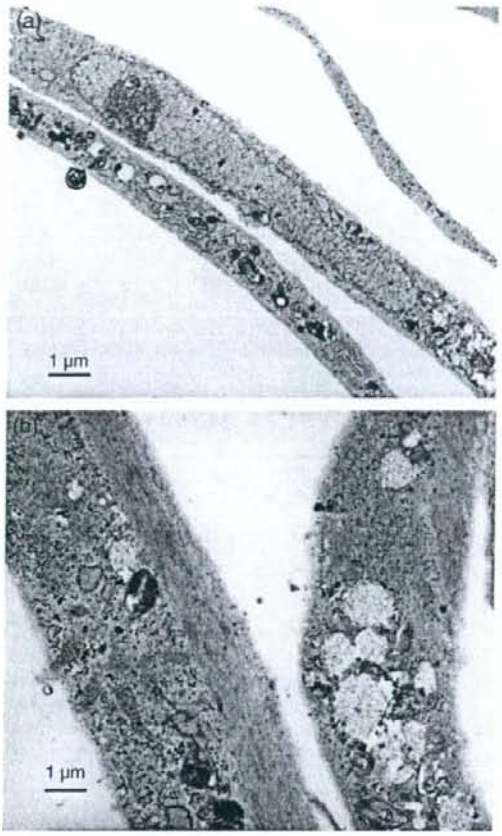

Figure 2 The ultrastructures of hMSCs when keloid-derived fibroblasts were placed in the lower chamber in the dual-chamber cell migration assay. The reverse side of transmission electron microscopy demonstrated ultrastructural differences among the treatments. (a) Conspicuous nucleoli in the elongated nuclei and microfilaments with dense bodies indicating contractive ability are found in the cell periphery. The cytoplasm developed a rough endoplasmic reticulum (×5000). (b) The high-power view demonstrated evident microfilaments with dense bodies of contractile filaments similar to those observed in myofibroblasts or smooth muscle cells (×10,000)

In the next step, to clarify either cell–cell or humoral interaction with keloid-derived fibroblasts, ultrastructural analyses with both a 3-μm pore membrane and direct monolayer coculture demonstrated hMSC cellular changes toward cell differentiation, especially cytoplasmic structural changes toward myofibroblasts. Collagen fiber bundles were expressed and secreted in the dual-chamber assay, and the cell morphology changed even more to myofibroblasts with

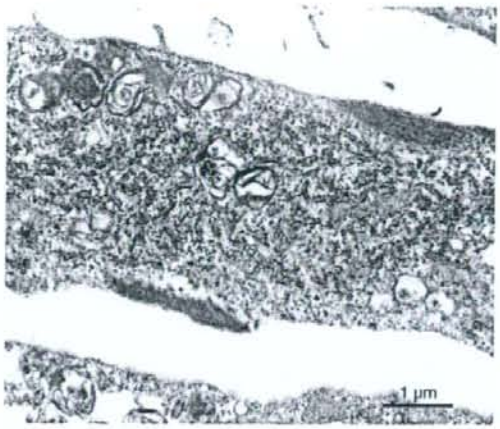

Figure 3 Monolayer coculture of hMSCs and keloid-derived fibroblasts (×10,000). The direct coculture of keloid-derived fibroblasts and hMSCs demonstrated more progressed myofibroblastic changes, characterized by cytoplasmic differentiation as depicted by abundant rough endoplasmic reticulum and the secretion of collagen-like fibers as well as actin-type microfilament bundles

abundant myofibers, rough endoplasmic reticulae and the secretion of collagen bundles. As a feature of predominant "myofibroblasts" in the keloid,[13] our data supported these characteristics as well as the invasion observed in IGF-I pathways[2] observed in the cell migration assay. Taken together, hMSCs are able to migrate into sites where keloid fibroblasts exist and may contribute to keloid pathogenesis as demonstrated by rich collagen production in the cytoplasms of hMSCs observed in both dual and direct coculture systems. The hMSCs are able to interact with other cells *in vitro* as previously demonstrated in a dual-chamber migration study,[12] and, furthermore, this study confirmed that the hMSCs are able to induce extracellular matrices when cocultured with keloid fibroblasts. In addition, this is the first evidence that keloid fibroblasts or keloid-derived humoral factors induced the hMSC differentiation although lipid mediators demonstrated the hMSC differentiation.[7] Keloid-derived fibroblasts demonstrated significantly abundant fibronectin expression with hMSCs in the upper chamber. This suggests that hMSCs participate in keloid formation by producing extracellular matrices and, thus, cause the extension and exaggeration of keloid formation. These phenomena may be implicated in the recurrence of keloids in the same area or the exacerbation of preexisting keloids through the bloodstream, since good reproducible animal models are established for the investigation of keloid recurrence and extension.

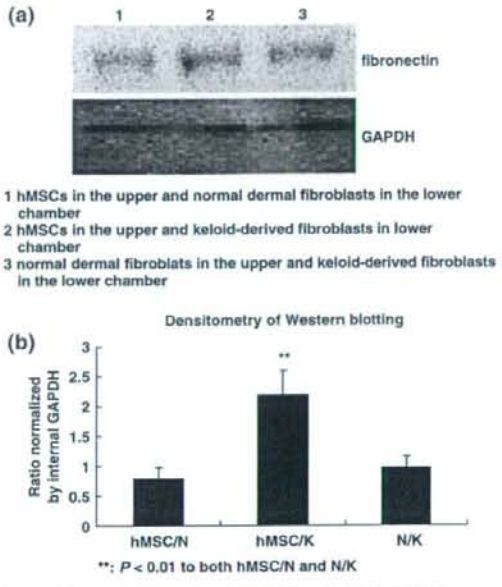

Figure 4 Fibronectin Western blot analysis from the dual-chamber incubation for 24 h. (a) Blotting demonstrated each combination of the cells (top) and internal GAPDH expression (bottom). The extracts were obtained from the bottom plates. (b) Densitometic analysis of each combination of the cells which is normalized by internal GAPDH expression. Five-time calculation of each band densitometry was statistically compared. When hMSCs were plated in the upper and keloid-derived fibroblasts in the lower chamber, there were significant differences compared to the others ($P > 0.01$)

Acknowledgment

This study was supported by grants from the Japanese Ministry of Education, Sports and Culture (nos 16390511, 16591795, 16659487, 16791091, 17659562, 17659563, 18390478, 18591967 and 18659526).

References

1 Peltonen J, Hsiao LL, Jaakkola S, *et al.* Activation of collagen gene expression in keloids: co-localization of type I and type VI collagen and transforming growth factor-β1 mRNA. *J Invest Dermatol* 1991; 97: 240–248.
2 Yoshimoto H, Ishihara H, Ohtsuru A, *et al.* Overexpression of insulin-like growth factor-1 (IGF-1) receptor and the invasiveness of cultured keloid fibroblasts. *Am J Pathol* 1999; 154: 883–889.
3 Haisa M, Okochi H, Grotendorst GR. Elevated levels of PDGFα receptors in keloid fibroblasts contribute to an enhanced response to PDGF. *J Invest Dermatol* 1994; 103: 560–563.
4 Tuan TL, Wu H, Huang EY, *et al.* Increased plasminogen activator inhibitor-1 in keloid fibroblasts may account for their elevated collagen accumulation in fibrin gel cultures. *Am J Pathol* 2003; 162: 1579–1589.
5 Rahban SR, Garner WL. Fibroproliferative scars. *Clin Plastic Surg* 2003; 30: 77–89.
6 Barry FP. Biology and clinical applications of mesenchymal stem cells. *Birth Defects Res C Embryo Today* 2003; 69: 250–256.
7 Akino K, Mineda T, Mori N, *et al.* Attenuation of cysteinyl leukotrienes induces human mesenchymal stem cell differentiation. *Wound Repair Regen* 2006; 14: 343–349.
8 Daian T, Ohtsuru A, Rogounovitch T, *et al.* Insulin-like growth factor-I enhances transforming growth factor-β-induced extracellular matrix protein production through the p38/activating transcription factor-2 signaling pathway in keloid fibroblasts. *J Invest Dermatol* 2003; 120: 956–962.
9 Yamamoto T, Takagawa S, Katayama I, *et al.* Anti-sclerotic effect of transforming growth factor-β antibody in a mouse model of bleomycin-induced scleroderma. *Clin Immunol* 1999; 92: 6–13.
10 Ortiz LA, Gambelli F, McBride C, *et al.* Mesenchymal stem cell engraftment in lung is enhanced in response to bleomycin exposure and ameliorates its fibrotic effects. *Proc Natl Acad Sci USA* 2003; 100: 8407–8411.
11 Akino K, Mineta T, Fukui M, *et al.* Bone morphogenetic protein-2 regulates proliferation of human mesenchymal stem cells. *Wound Repair Regen* 2003; 11: 354–360.
12 Akino K, Mineda T, Akita S. Early cellular changes of human mesenchymal stem cells and their interaction with other cells. *Wound Repair Regen* 2005; 13: 434–440.
13 Santucci M, Borgognoni L. Keloids and hypertrophic scars of Caucasians show distinctive morphologic and immunophenotypic profiles. *Virchows Arch* 2001; 438: 457–463.

4. 創傷治癒に関与する細胞増殖因子

秋田定伯*　平野明喜*

Key words：細胞増殖因子の発現・作用様式・標的　各種細胞増殖因子の特徴

はじめに

創傷治癒過程における，細胞増殖因子の役割は，受傷直後からの炎症細胞，線維芽細胞，血管内皮細胞などへ直接的，間接的に作用して，創傷治癒を促進することである。創傷治癒の各相で主要な役割を演じる細胞発現時期は重複した時期があり，複合的作用を呈する場合がある。

I. 経時的な細胞増殖因子の発現・作用様式

受傷直後から血小板が活性化され，出血対策，ホメオスターシス維持を目的として凝血形成・凝固カスケードが促進され，トロンビン，フィブリン，補体などを刺激合成する。また，血小板 α 顆粒に存在する血管内皮細胞増殖因子（vascular endothelial growth factor；VEGF），トランスフォーミング細胞増殖因子-α（transforming growth factor-α；TGF-α），TGF-βなどの細胞増殖因子を一酸化窒素（nitric oxide；NO），プロスタグランディンなどとともに活性化する。受傷後から数時間は，好中球，多核白血球が凝固部位に集合し，血管拡張作用により，好中球は間質に漏出し，炎症性蛋白とともに浮腫を来たす。この好中球の一連の作用としてプロテアーゼ，フリーラジカルなどによって代謝物，病原体を食作用により排出する。細胞に伝達するシグナルは単核球を受傷後 2～4 日に活性化マクロファージへと転換する。マクロファージはフリーラジカルの産生，血管拡張，食作用をさらに増強しつつ，受傷後 5 日からの増殖期に重要な橋渡しとなる。

活性化マクロファージは VEGF，TGF-α，線維芽細胞増殖因子（fibroblast growth factor；FGF）を活性化し血管形成と血管新生を促進する。結合織形成，線維形成は線維芽細胞から産生される上皮細胞増殖因子（epidermal growth factor；EGF），血小板由来細胞増殖因子（platelet-derived growth factor；PDGF），TGF-β，腫瘍壊死因子-α（tumor necrosis factor-α；TNF-α），インターロイキン-1（interleukin-1；IL-1），NO などより一次マトリックスを形成する。白血球プロテアーゼは凝集塊・凝血塊を融解し細胞遊走性亢進とコラーゲンによる細胞外マトリックスを構成しはじめ，肉芽形成が開始する。ウイルス，真菌，細菌の堆積物はマクロファージによる食作用によって抗原呈示し[1] B 細胞産生による抗体産生と特異的 T 細胞による食作用を引き起こす。線維芽細胞と血管内皮細胞は増殖期における T 細胞による制御の主要細胞である。さらに，マクロファージ産生

*長崎大学大学院医歯薬学総合研究科形成外科